Supporting Information

1. Kramers-Kronig Transformation and Refractive Index of $Ru(bpy)_3^{2+}$

The LSPR shift is dependent on the refractive index of the surrounding medium of the nanoparticle. For non-resonant adsorbates, the LSPR wavelength shift ($\Delta\lambda_{max}$) can be estimated from the following empirical equation:[1-4]

$$\Delta\lambda_{max} = m(n_{ads} - n_{N_2})(1 - e^{-2d/l_d}) \qquad \text{(S1)}$$

where m is the refractive index sensitivity of the nanoparticles (~200 nm/RIU),[1, 5] n_{ads} is the real part of the refractive index of the adsorbate, n_{N_2} is the refractive index of the N_2 surroundings (1.0), d is the molecular thickness (1.5 nm for $Ru(bpy)_3^{2+}$), and l_d is the characteristic electromagnetic field decay length of the nanoparticles (approximately 6 nm).[1]

For resonant adsorbates, it has been demonstrated that $\Delta\lambda_{max}$ near molecular resonance can be estimated from the real part of the refractive index (using a Kramers-Kronig transformation[6]) and Eq. S1. Using the same treatment as in the previous studies, n_{ads} is expressed as the sum of the nonresonant part of the refractive index ($n_{non,ads}$) and the resonant contribution ($\Delta n_{res,ads}$). From Eq. S1, the refractive index of the adsorbate layer can be estimated. Since the average $\Delta\lambda_{max}$ at off-molecular resonance wavelengths is 10 nm, the $n_{non,ads}$ of $Ru(bpy)_2^{3+}$ is calculated to be ~ 1.1.

Using a Kramers-Kronig transformation, $\Delta n_{res,ads}$ of $Ru(bpy)_2^{3+}$ was transformed from its solution absorption spectrum using the following equation:[6, 7]

$$\Delta n_{res,ads}(\omega) = \frac{c}{\pi}\int_0^{\infty} \frac{\Delta\alpha(\omega')}{(\omega')^2 - \omega^2} d\omega' \qquad \text{(S2)}$$

where $\Delta\alpha$ is the change in the absorption coefficient ($2.303 * A(\lambda)/T$ in which $A(\lambda)$ is the molecular absorbance at a given wavelength and T is the effective molecular thickness), c is the

speed of light, λ is the wavelength of light, and ω is the angular frequency ($2\pi c/\lambda$). The Kramers-Kronig transformation expresses the real part of the refractive indices as an integral of the absorption coefficients. From the LSPR shift measurements, only the electronic transition of $Ru(bpy)_3^{2+}$ at 452 nm couples strongly to the LSPR. To get the dielectric constant corresponding to electronic transition of $Ru(bpy)_3^{2+}$ at 452 nm, the absorption spectrum was deconvoluted with two Gaussian curves at 452 nm and 425 nm. Kramers-Kronig transformation was performed with the 452 nm Gaussian curve (Figure S1). Notice that the integral in this formula has a singularity, which was treated numerically by excluding the singular point in the integral. And in the Kramers-Kronig transformation, the integration is from 0 to infinite frequency where in the experiments, only information over certain frequency ranges is available. In addition, $Ru(bpy)_2^{3+}$ has strong electronic resonances in the UV which will contribute significantly to its dielectric constants but are neglected in the current application. This treatment will lead to some uncertainty in the absolute value of the refractive indices.

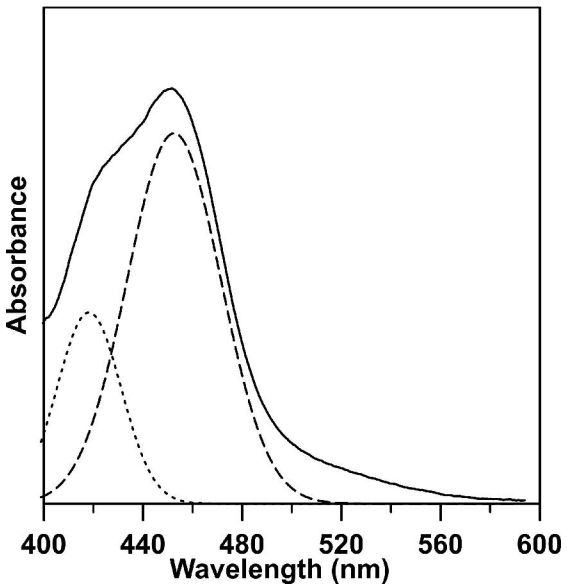

Figure S1 Deconvolution of the absorption band of $Ru(bpy)_3^{2+}$.

2. Extinction Cross-Section of Bare and Layered Spheroid, Including Radiation Damping Effects

For a prolate spheroid oriented along the z direction ($\frac{x^2+y^2}{a^2}+\frac{z^2}{b^2}=1$, $a<b$), parallel to the direction of the applied electric field, in the quasistatic limit where the dimension of a

spheroid is much smaller than the incident wavelength, the parallel component of polarizability of the spheroid is[7-9]

$$\alpha = \frac{1}{3} f^3 \frac{\xi_0}{Q_1(\xi_0)} \left\{ \frac{\varepsilon_i - \varepsilon_o}{\varepsilon_i + \chi \varepsilon_o} \right\} \qquad \text{(S3)}$$

where ε_0 is the dielectric constant of the medium outside the spheroid (N_2 in this work), ε_i is the dielectric function of the spheroid (Ag in this work), and f is the focus of the spheroid given by:

$$f = (b^2 - a^2)^{1/2} \qquad \text{(S4)}$$

ξ_0 is the value of ξ at the spheroid surface where:

$$\xi_0 = \frac{1}{\sqrt{1 - \frac{a^2}{b^2}}} \qquad \text{(S5)}$$

Q_1 is a Legendre function of the second kind where:

$$Q_1(\xi_0) = \frac{\xi_0}{2} \ln\left(\frac{\xi_0 - 1}{\xi_0 + 1}\right) - 1 \qquad \text{(S6)}$$

and the function χ is given by:

$$\chi = -1 + \frac{1}{(\xi_0^{\,2} - 1) Q_1(\xi_0)} \qquad \text{(S7)}$$

The extinction cross section (C_{ext}) of a spheroid is proportional to the imaginary part of its porlarizability:

$$C_{ext} \propto \frac{1}{\lambda} \mathrm{Im}(\alpha) \propto \frac{1}{\lambda} \mathrm{Im}\left\{ \frac{\varepsilon_i - \varepsilon_o}{\varepsilon_i + \chi \varepsilon_o} \right\} \qquad \text{(S8)}$$

For a spheroid coated with a layer, the parallel component of its polarizability becomes[8]

$$\alpha = \frac{f^3}{3} \left\{ \frac{\xi_1}{Q_1(\xi_1)} (G - 1) - \frac{\xi_0}{Q_1(\xi_0)} \frac{\varepsilon_i - \varepsilon_l}{\varepsilon_i + \chi \varepsilon_l} G \right\} \qquad \text{(S9)}$$

where

$$G = \frac{\xi_1 - \dfrac{Q_1(\xi_1)}{Q_1'(\xi_1)}}{\left(\dfrac{\varepsilon_l}{\varepsilon_o}\dfrac{Q_1(\xi_1)}{Q_1'(\xi_1)} - \xi_1\right) + \dfrac{(1-\dfrac{\varepsilon_l}{\varepsilon_o})(1-\dfrac{\varepsilon_l}{\varepsilon_i})Q_1(\xi_1)}{\left(\dfrac{Q_1(\xi_o)}{\xi_o} - \dfrac{\varepsilon_l}{\varepsilon_i}Q_1'(\xi_o)\right)}} \qquad \text{(S10)}$$

Here ε_l is the dielectric constant of the layer ($Ru(bpy)_3^{2+}$ for this work), ξ_0 and ξ_1 are the value of ξ at the inner and outer surface of the layered spheroid using spheroidal coordinates. G is a correction factor that comes from solving the LaPlace equation for the layered spheriod. The extinction cross section becomes:

$$C_{ext} \propto \frac{1}{\lambda}\,\mathrm{Im}\left\{\frac{\xi_1}{Q_1(\xi_1)}(G-1) - \frac{\xi_0}{Q_1(\xi_0)}\frac{\varepsilon_i - \varepsilon_l}{\varepsilon_i + \chi\varepsilon_l}G\right\} \qquad \text{(S11)}$$

To correct the static result for radiation damping and depolarization, we used the approach developed by Meier et.al.[10] for spheres and generalized by Zeman et. al. for spheroids.[11].

$$D = (1 - \frac{2}{3}ik^3\alpha - k^2\alpha/b)^{-1} \qquad \text{(S12)}$$

where $k = \varepsilon_0^{1/2}\omega/c$. Let $\gamma_0 = \dfrac{\varepsilon_i - \varepsilon_o}{\varepsilon_i + \chi\varepsilon_o}$ for the bare spheroid and $\gamma_1 = \dfrac{\varepsilon_i - \varepsilon_l}{\varepsilon_i + \chi\varepsilon_l}$ for the layered spheroid. The incorporation of Eq. S12 is accomplished by replacing γ_0 and γ_1 by $D\gamma_0$ and $D\gamma_1$ wherever it appears. Using Eq. S8 and S11, we calculate the extinction of a bare Ag spheroid and that coated with a layer of $Ru(bpy)_3^{2+}$ in N_2. Figure S2 shows the calculated extinction spectra of bare (solid lines) and $Ru(bpy)_3^{2+}$-coated (dashed lines) Ag spheroids. Here the extinction wavelength of the Ag spheroid is varied by varying χ. Each pair of spectra with the same colors is calculated using the same χ. Notice that there is a dip in the extinction spectrum of the layered Ag spheroid due to $Ru(bpy)_3^{2+}$ absorption, and the extinction splits into two bands.

This extinction lineshape change has been reported by several groups with the experimental and theoretical studies for a resonant molecule interacting with Au nanospheres or nanorods.[12-14] However, in our experiments, no significant change is observed in the extinction of the Ag nanoparticles after $Ru(bpy)_3^{2+}$ adsorption other than a wavelength shift. This indicates that in the experiments, the absorbance of $Ru(bpy)_3^{2+}$ is relatively small compared to the extinction of the Ag nanoparticles; therefore, the effect of the $Ru(bpy)_3^{2+}$ layer on the LSPR is to produce a spectral shift but not a lineshape change. In the modeling, this effect is much more significant in both the spectra shift and line shape change.

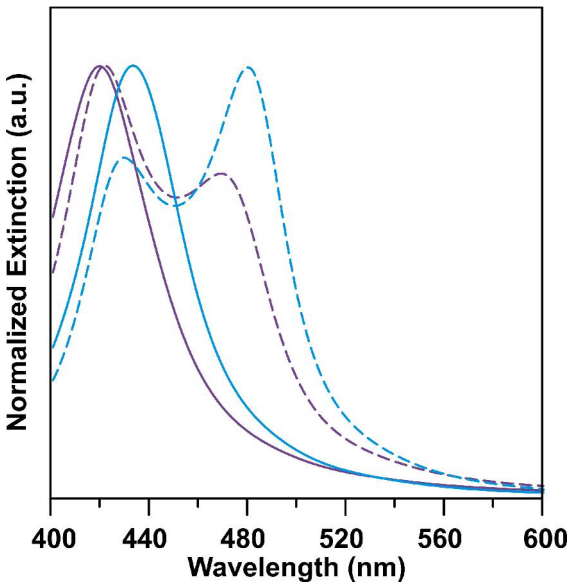

Figure S2. Calculated extinction spectra of bare Ag spheroid (solid lines) and Ag spheroid with $Ru(bpy)_3^{2+}$ (dashed lines) with varying χ parameters. Each pair of spectra of the same color was calculated with the same χ.

3. Square of the Average Electric Field of Bare and Layered Spheroid

For a spheroid, the average of the square of the electric field over the spheroid surface is expressed by the following equation

$$\left\langle |E|^2 \right\rangle = \left\langle |E_0|^2 \right\rangle \left\{ |1-\gamma_0|^2 + \left[\frac{2\,\mathrm{Re}(1-\gamma_0)\gamma_0^*}{Q_1(\xi_0)} + \frac{\gamma_0^{\,2}}{Q_1^{\,2}(\xi_0)(\xi_0^{\,2}-1)} \right] \left(\frac{-\sqrt{\xi_0^{\,2}-1} + \xi_0^{\,2} \sin^{-1}\frac{1}{\xi_0}}{\sqrt{\xi_0^{\,2}-1} + \xi_0^{\,2} \sin^{-1}\frac{1}{\xi_0}} \right) \right\} \quad \text{(S13)}$$

For the layered spheroid, the average of the square of the electric field over the surface within the layer ($\xi_0 \le \xi \le \xi_1$) is[8]

$$\left\langle |E|^2 \right\rangle = |E_0|^2 |G|^2 \left\{ |B|^2 + \left[\frac{2\,\mathrm{Re}(B)A^*}{\xi} + \frac{|A|^2}{\xi^2(\xi^2-1)} \right] \left(\frac{-\sqrt{\xi^2-1} + \xi^2 \sin^{-1}\frac{1}{\xi}}{\sqrt{\xi^2-1} + \xi^2 \sin^{-1}\frac{1}{\xi_0}} \right) \right\}^2 \qquad \text{(S14)}$$

$$A = \gamma_1 \frac{\xi_0}{Q_1(\xi_0)} \qquad \text{(S15)}$$

$$B = 1 - A\frac{Q_1(\xi)}{\xi} \qquad \text{(S16)}$$

When the layer is thin, the electric field within the layer does not change with different ξ values. Therefore, we use the electric field at the outer surface to represent the average electric field in the layer. Figure S3 shows $\left\langle |E|^2 \right\rangle / |E_0|^2$ versus wavelength at the surface of the spheroid without (solid line) and with (dashed line) a layer of $Ru(bpy)_3^{2+}$ with the same size and aspect ratio.

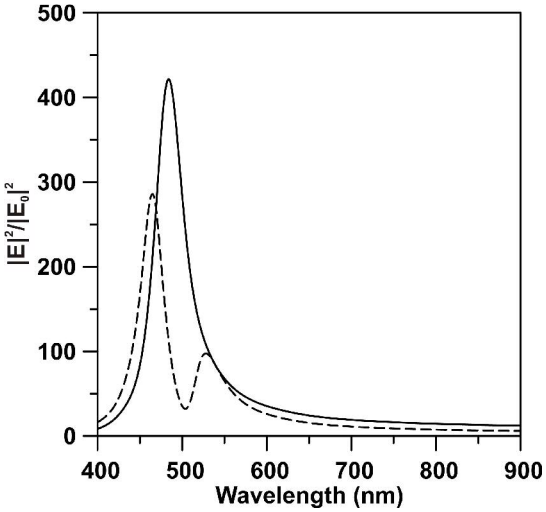

Figure S3. Calculated $\left\langle |E|^2 \right\rangle / |E_0|^2$ of a bare Ag spheroid (solid lines) and Ag spheroid with $Ru(bpy)_3^{2+}$ (dashed lines) with the same χ parameter.

The absorption of the layer of $Ru(bpy)_3^{2+}$ leads to a decrease in the magnitude of $\left\langle |E|^2 \right\rangle / |E_0|^2$ and a dip in the $\left\langle |E|^2 \right\rangle / |E_0|^2$ profile. As stated in the second section of the Supporting Information, this model overestimates the effect of the resonant layer in both extinction spectral shape and the electric field profile. Therefore, a bare spheroid model is used to simulate the average electric field around the nanoparticles that are used in the experiments.

4. **An Example SERRS EF Calculation**

Since the intensity observed in the SERRS spectrum of $Ru(bpy)_3^{2+}$ can be interpreted as the normal Raman scattering cross section multiplied by the resonance Raman and EM enhancement factors, it is possible to write an expression for a decoupled SERRS enhancement factor.

McFarland et al[15] gives an expression for the non-resonant EF for the case where the SERS and normal Raman analyte are the same molecule, eliminating the need to normalize by differing cross-sections. In the present work, it is difficult to observe the magnitude of the resonance Raman intensity due to fluorescence. Therefore, the normal Raman intensity is given for a non-resonant molecule and the EF expression must include a cross-section normalization. The expression for the overall decoupled SERRS EF is:

$$EF_{SERRS} = \frac{I_{SERRS,Ru} \Big/ \left(N_{SERRS,Ru} \cdot \sigma_{NR,Ru} \right)}{I_{NR,Cyc} \Big/ \left(N_{NR} \cdot \sigma_{NR,Cyc} \right)} \qquad \text{(S17)}$$

where I, N and σ are the intensities, number of and cross-sections of the resonance Raman (RR) and normal Raman (NR) analytes, respectively. By normalizing the observed SERRS intensity to the resonant $Ru(bpy)_3^{2+}$ cross-section, the EF_{SERRS} term only corresponds to EM enhancement. The measured intensities for the sample in Figure 5.8E were I_{SERRS} = 30.82 cts mW^{-1} s^{-1} for $Ru(bpy)_3^{2+}$ 1487 cm^{-1} mode and I_{NR} = 20.82 cts mW^{-1} s^{-1} for cyclohexane 1444.4 cm^{-1} mode at λ_{ex} = 465 nm. Comparing the intensity of the 1487 cm^{-1} $Ru(bpy)_3^{2+}$ mode to the 983 cm^{-1} SO_4^{2+} mode measured by Mallick et. al. [16], and using the SO_4^{2+} cross section of 14.8 x 10^{-30} at λ_{ex} = 465 nm as internal standard,[17] the resonant cross section of $Ru(bpy)_3^{2+}$ was determined to be σ_{RRS} = 4.4 x 10^{-26} cm^2 $molecule^{-1}$ at λ_{ex} = 465 nm. The normal Raman cross section for the 1444.4 cm^{-1} cyclohexane mode was determined to be σ_{NR} = 9.37 x 10^{-30} cm^2 $molecule^{-1}$ at λ_{ex} = 465 nm after correcting for ν^4.[18] The number of $Ru(bpy)_3^{2+}$ molecules present in the probe volume was determined to be N_{SERRS} = 1.8 x 10^5 assuming a surface coverage of 0.65x10^{14} molecules cm^{-2} from the electrochemistry measurement, a 4 μm^2 laser spot size and only 7% coverage of nanoparticles resulting from NSL.[19] The number of cyclohexane molecules was estimated to be N_{NR} = 2.4 x 10^{12}. This was found by assuming that the probe volume was a

cylinder of 100 μm in length with 4 μm^2 cross-section and using its bulk density of 6.0 x 10^{17} molecules cm^{-2} μm^{-1}. Using these numbers, the EM EF was determined to be 4.16 x 10^3. Assuming that the resonant Raman EF is on the order of 40,[20] the overall EF observed here is 1.66 x 10^5.

REFERENCES

1. Haes, A. J.; Hall, W. P.; Chang, L.; Klein, W. L.; Van Duyne, R. P., *Nano Lett.* **2004,** *4*.
2. Haes, A. J.; Zou, S. L.; Zhao, J.; Schatz, G. C.; Van Duyne, R. P., *J Am Chem Soc* **2006,** *128*.
3. Riboh, J. C.; Haes, A. J.; McFarland, A. D.; Yonzon, C. R.; Van Duyne, R. P., *J. Phys. Chem. B* **2003,** *107*.
4. Jung, L. S.; Campbell, C. T.; Chinowsky, T. M.; Mar, M. N.; Yee, S. S., *Langmuir* **1998,** *14*.
5. Malinsky, M. D.; Kelly, K. L.; Schatz, G. C.; Van Duyne, R. P., *J. Am. Chem. Soc.* **2001,** *123*.
6. Kronig, R. d. L.; Kramers, H. A., *Zeitschrift fuer Physik* **1928,** *48*.
7. Huffman, C. F. B. a. D. R., *Absorption and Scattering of Light by Small Particles*. Wiley Interscience: New York, 1983.
8. Zeman, E. J.; Carron, K. T.; Schatz, G. C.; Vanduyne, R. P., *J. Chem. Phys.* **1987,** *87*, 4189.
9. Gersten, J.; Nitzan, A., *J. Chem. Phys.* **1980,** *73*, 3023.
10. Meier, M.; Wokaun, A., *Optics Letters* **1983,** *8*, 581.
11. Zeman, E. J.; Schatz, G. C., *J. Phys. Chem.* **1987,** *91*, 634.
12. Wiederrecht, G. P.; Wurtz, G. A.; Hranisavljevic, J., *Nano Lett* **2004,** *4*, 2121.
13. Wurtz, G. A.; Evans, P. R.; Hendren, W.; Atkinson, R.; Dickson, W.; Pollard, R. J.; Zayats, A. V.; Harrison, W.; Bower, C., *Nano Lett* **2007,** *7*, 1297.
14. Kelley, A. M., *Nano Lett* **2007,** *7*, 3235.
15. McFarland, A. D.; Young, M. A.; Dieringer, J. A.; Van Duyne, R. P., *J. Phys. Chem. B* **2005,** *109*, 11279.
16. Mallick, P. K.; Danzer, G. D.; Strommen, D. P.; Kincaid, J. R., *J. Phys. Chem.* **1988,** *92*, 5628.
17. Dudik, J. M.; Johnson, C. R.; Asher, S. A., *J. Chem. Phys.* **1985,** *82*, 1732.
18. Trulson, M. O.; Mathies, R. A., *J. Chem. Phys.* **1986,** *84*, 2068.
19. Haynes, C. L.; Van Duyne, R. P., *J. Phys. Chem. B* **2001,** *105*, 5599.
20. Haynes, C. L.; Van Duyne, R. P., *J. Phys. Chem. B* **2003,** *107*, 7426.